Organic & Biomolecular Chemistry

ROYAL SOCIETY OF CHEMISTRY

PAPER

View Article Online
View Journal | View Issue

Cite this: *Org. Biomol. Chem.*, 2021, **19**, 387

Kinetic and structure–activity studies of the triazolium ion-catalysed benzoin condensation†

Richard S. Massey,[a] Jacob Murray,[a] Christopher J. Collett,[b] Jiayun Zhu,[a] Andrew D. Smith[b] and AnnMarie C. O'Donoghue*[a]

Received 5th November 2020,
Accepted 11th December 2020

DOI: 10.1039/d0ob02207a

rsc.li/obc

Steady-state kinetic and structure–activity studies of a series of six triazolium-ion pre-catalysts **2a–2f** were investigated for the benzoin condensation. These data provide quantitative insight into the role of triazolium *N*-aryl substitution under synthetically relevant catalytic conditions in a polar solvent environment. Kinetic behaviour was significantly different to that previously reported for a related thiazolium-ion pre-catalyst **1**, with the observed levelling of initial rate constants to ν_{max} at high aldehyde concentrations for all triazolium catalysts. Values for ν_{max} for **2a–2f** increase with electron withdrawing *N*-aryl substituents, in agreement with reported optimal synthetic outcomes under catalytic conditions, and vary by 75-fold across the series. The levelling of rate constants supports a change in rate-limiting step and evidence supports the assignment of the Breslow-intermediate forming step to the plateau region. Correlation of ν_{max} reaction data yielded a positive Hammett ρ-value (ρ = +1.66) supporting the build up of electron density adjacent to the triazolium *N*-Ar in the rate-limiting step favoured by electron withdrawing *N*-aryl substituents. At lower concentrations of aldehyde, both Breslow-intermediate and benzoin formation are partially rate-limiting.

Introduction

N-Heterocyclic carbenes (NHCs) have made a major impact on the field of catalysis and are arguably one of the most versatile, efficient classes of organocatalyst. Recent synthetic advances include the development of high yielding, stereoselective NHCs; a strong drive to carry out catalytic reactions in more sustainable, aqueous conditions; and implications in the fields of bio- and enzymatic catalysis.[1] A key reaction at the centre of NHC-catalysis is the benzoin condensation (Scheme 1), in which the catalyst facilitates polarity reversal (umpolung) of an aldehyde, enabling nucleophilic reaction at a second aldehyde molecule.[1a] The benzoin reaction is often the test reaction of choice in evaluating new NHC-catalyst scaffolds. Despite broad interest, there remain many mechanistic ambiguities with respect to NHC-catalysed processes including the benzoin reaction. Since the seminal mechanistic studies of the benzoin reaction by Breslow (Scheme 1), the existence of the enaminol, or Breslow intermediate (**IV**), has been the focus of much research and debate.[2] Computational studies, including work by Houk and others, have provided *ab initio* evidence for the Breslow intermediate, whilst also predicting experimentally observed product outcomes.[3] Mechanistic studies have mainly focussed on isolation of **IV**; this initially included the isolation in 2012 of aza-Breslow intermediates (**IV′**) and *O*-methylated derivatives (**IV″**) by Rovis

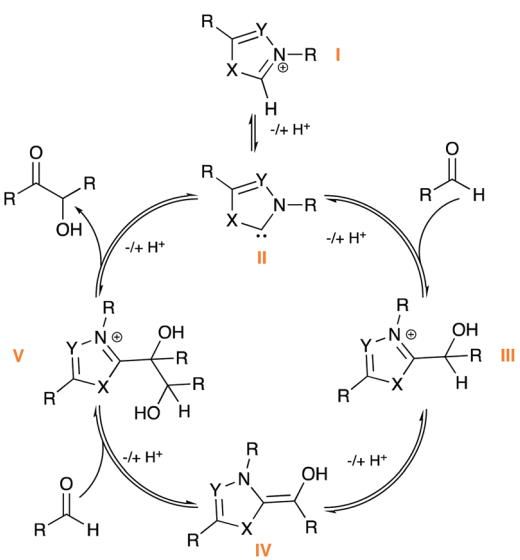

Scheme 1 The NHC-catalysed benzoin condensation, with key intermediates highlighted.

[a]*Department of Chemistry, Durham University, South Road, Durham DH1 3LE, UK. E-mail: annmarie.odonoghue@durham.ac.uk*
[b]*EaStCHEM, School of Chemistry, University of St. Andrews, North Haugh, St Andrews KY16 9SY, UK*

†Electronic supplementary information (ESI) available: Synthetic and kinetic methods; kinetic data fitting and analysis. See DOI: 10.1039/d0ob02207a

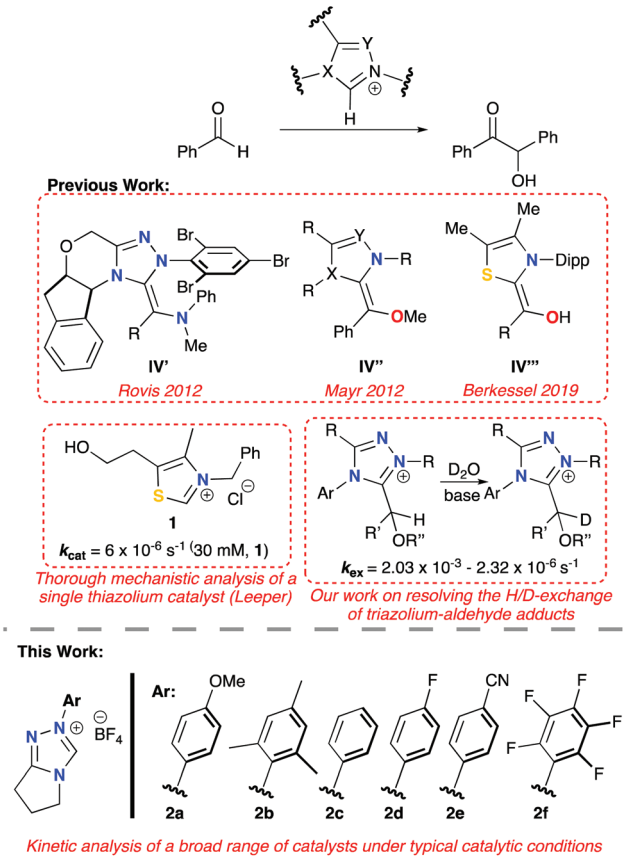

Fig. 1 Previous mechanistic studies of the NHC-catalysed benzoin condensation and the catalysts studied in this work.

and Mayr, respectively (Fig. 1).[4] In a series of seminal publications since 2012, Berkessel and co-workers reported the NMR and/or X-ray structural characterisation of unmodified **IV**, for imidazolyl, imidazolinyl and thiazolyl-derived NHCs (*e.g.* **IV'''**, Fig. 1).[5] Isolation and characterisation of unmasked, synthetically relevant Breslow intermediates of triazolium ions are yet to be reported and remain a key target in the field of NHC catalysis.

In terms of triazolium catalysis, our groups have reported the isolation and structural characterisation of a series of triazolium-derived adducts (**III**; X = Y = N) and demonstrated that (**III**) form reversibly from free aldehyde and triazolium pre-catalyst. Kinetic analysis of the H/D-exchange reactions at the α-position enabled structural effects on Breslow intermediate formation from (**III**) to be directly assessed (Fig. 1). Stoichiometric studies provided access to rate constants for initial adduct (**III**) formation and decay from triazolium pre-catalyst.[6] An earlier study by Huskey and Jordan reported a related kinetic analysis of thiazolium-aldehyde adducts and the determination of a C(α)–H pK_a of 15.7 for one example.[7] To date, there has been no report of experimental adduct (**III**) C(α)–H pK_a values for the triazolyl series.

Regarding detailed kinetic analysis of the overall NHC-catalysed benzoin reaction, integrated-rate analyses from various studies gave different and often ambiguous results, with all studies mainly focusing on thiazolium catalysis (**I**; X = S, Y = C).[2b,8] Key issues in these investigations include the observation that the reaction order changes with the concentration of benzaldehyde ([PhCHO]); catalyst concentration is not necessarily constant due to degradation; concentration of base can be affected by formation of benzoic acid side-product over time; and finally, the assumption of irreversibility is not always appropriate. For enzymatic processes, which suffer from similar problems, kineticists employ an initial rate method (IRM) at low % product conversion to circumvent these issues. Importantly, Leeper and co-workers reported an IRM screening of thiazolium catalyst **1**, under true catalytic conditions (Fig. 1), reporting a first-order dependence on [PhCHO], with a pseudo-first order rate constant, $k_{cat} = 6 \times 10^{-6}$ s^{-1}. Three rate-limiting scenarios were considered: (i) adduct (**III**) formation; (ii) Breslow intermediate (**IV**) formation; (iii) attack of **IV** to a second PhCHO (Scheme 1). Further stoichiometric studies and deuterium labelling determined that all three stages of the process must be in-part rate-limiting to account for all the observations. At higher concentrations of benzaldehyde, rate is more limited by deprotonation to form **IV** (k_{BI}); conversely, at reduced concentrations of benzaldehyde, the initial adduct and product-forming steps are considered to be more rate-limiting.[9]

Leeper's IRM and stoichiometric studies of the thiazolium-catalysed mechanism highlight the importance of rigorous understanding of the kinetics of catalytic processes. Knowledge of the rate-limiting processes within a reaction allow for targeted development of catalysts for improved methods. Moreover, as the push towards aqueous organocatalysis increases, detailed mechanistic understanding of key rate-limiting factors will aid catalytic development for a more synthetically challenging environment.[1b,c] 1,2,4-Triazolium ions are often the preferred NHC catalysts due to increased propensities for functionalization and therefore stereoselectivity, but also increased activities.[1a] pK_a values of triazoliums are 1–3 units lower than their thiazolium relatives, correlating to enhanced rates within the benzoin reaction.[6a,10]

Despite the widespread application of 1,2,4-triazolium ions in contemporary organocatalysis, quantitative kinetic insights into the triazolium-catalysed benzoin condensation are limited. Herein, we report an IRM-study of the triazolium catalysed reaction, under true catalytic conditions, and a structure–activity study of reaction data. A polar, protic MeOH environment was chosen for kinetic analysis, to enable comparison with the previous thiazolium ion study by Leeper. Our results build upon our previous stoichiometric triazolium catalyst studies providing quantitative insight of the interplay of structure and kinetic activity for these commonly-used organocatalyst systems.[9]

Results and discussion

Initial work focused on repetition of Leeper's work on commercially available thiazolium catalyst **1**, whose structure

resembles the enzymatic co-factor thiamine, and extension to a broader range of catalyst concentrations.[1a,9] Freshly distilled benzaldehyde (0.32–1.6 M) was added to triethylamine-buffered MeOH solutions of **1** (12, 24, 30 mM) at 50 °C. At regular intervals, aliquots of the reaction mixture were quenched with MeCN and both benzaldehyde and benzoin concentrations were quantified *via* HPLC. A first-order dependence on benzaldehyde concentration was observed at all concentrations of **1** (ESI, section S2, Fig. S13†). The pseudo-first-order rate constant, k_{cat}, is determined as the gradient of a plot of initial benzaldehyde concentration ($[PhCHO]_0$) against initial rate (ν, eqn (1)). Our value of $k_{cat} = 5.53 \times 10^{-6}$ s^{-1} for 30 mM pre-catalyst is in excellent agreement with Leeper's reported value.[9]

$$\nu = k_{cat}[PhCHO]^n \quad (1)$$

Using identical reaction conditions as employed for thiazolium salt **1** (triethylamine-buffered MeOH at 50 °C), triazolium pre-catalysts **2a–f** showed distinctly different kinetic behaviour. Triazolium pre-catalysts **2a–f** clearly demonstrate saturation kinetic profiles at higher benzaldehyde concentrations (*e.g.* Fig. 2 for **2c**; ESI, section 2, Fig. S14–18† for **2a–b**, **2d–f**). By contrast, saturation was not observed for plots of ν *versus* $[PhCHO]_0$ for **1** at 12, 24 and 30 mM thiazolium catalyst (ESI, Fig. S13†).

Initial rate data for **2a–f** were fit to a steady-state rate equation (eqn (2)), derived for the Breslow intermediate **IV** in Scheme 2, with the assumption that the concentration of adduct ([**III**]) was equal to that of catalyst ([**I**]). This assumption is validated by our previous kinetic NMR studies with stoichiometric aryl aldehyde and triazolium salt concentrations in the same triethylamine-buffered methanol medium, which showed that adduct (**III**) forms rapidly and reversibly from these reactants at 25 °C.[6b] These previous studies for a range of aryl aldehydes and triazolium catalysts included the stoichiometric kinetic analysis of **2a–d** and benzaldehyde, permitting access to rate and equilibrium constants for formation of (**III**).[6b] Half-lives ($t_{1/2}$) for adduct **III** formation at 25 °C could be calculated as ~670 s and ~16 s for the lowest and highest $[PhCHO]_0$, which would be predicted to be a minimum of ~10-fold lower again at 50 °C, and significantly smaller than the kinetic experiment measurement times employed in the initial rate analysis (ESI, section S4†). Using the experimental equilibrium constants for adduct formation determined under stoichiometric conditions, values for the percentage of free pre-catalyst (%*I*) at equilibrium can also be estimated (Table S14†). Under the catalytic conditions of the initial rate study with a 10–100 fold excess of benzaldehyde relative to pre-catalyst, the equilibrium significantly favours adduct. Additionally, the use of the IRM approach permits the assumption that the reverse reaction of benzoin is not significant under the reaction conditions.‡

$$\nu = \frac{k_p \nu_{max}[PhCHO]}{k_{-BI} + k_p[PhCHO]} = \frac{k_p k_{BI}[I][PhCHO]}{k_{-BI} + k_p[PhCHO]} \quad (2)$$

The experimental data under catalytic conditions fit well to eqn (2) and, at high $[PhCHO]_0$, the values for the initial rates plateau and approach ν_{max}. There is some deviation of data-points at the lowest $[PhCHO]_0$ perhaps owing to a more significant % of pre-catalyst **I** still present initially at the lowest excess of aldehyde. Uncertainties in ν_{max} were obtained from the kinetic fits and, with the exception of **2e**, are relatively small. The uncertainty for the ν_{max} value for **2e** is larger due to this system not reaching a final plateau at the highest benzaldehyde concentration employed. Table 1 summarises the kinetic constants obtained from the fit to eqn (2) for catalysts **2a–f** (ESI, section S2† for kinetic fits for **2a,b,d–f**). The absolute values of these kinetic parameters are unique to the triethylamine buffer system employed in methanol as solvent, however, their comparison allows the effects of structural changes of catalyst on individual reaction steps to be determined. Values for ν_{max} vary greatly depending on the catalyst, with a large 75-fold difference between the slowest **2a** and fastest **2f** triazolium catalysts, and the largest value observed for a *N*-pentafluorophenyl substituent. This highlights the importance of targeted tuning of the electronic nature of the *N*-aryl substituent for efficient catalysis.

The plateauing of initial rate plots with respect to $[PhCHO]_0$ confirms a change in order of reaction and therefore change in rate-limiting step. Using eqn (2), at high $[PhCHO]_0$ when $k_p[PhCHO] \gg k_{-BI}$, values for ν_{max} approach $k_{BI}[I]$ *i.e.* deproto-

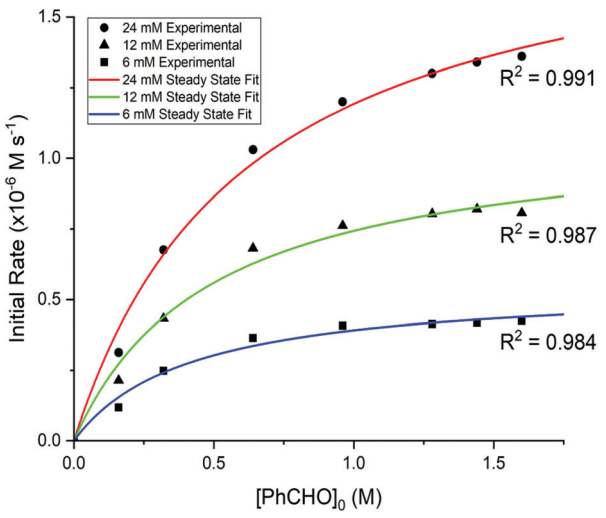

Fig. 2 Triazolium catalysis of the benzoin condensation under catalytic conditions at 50 °C: initial rate (ν, M s^{-1}) plot for **2c** at 24 (red), 12 (green) and 6 (blue) mM catalyst loading. The solid lines show the fit of the reaction data to eqn (2).

‡The IRM was chosen, with the reaction followed to <10% product formation, to minimize any contribution of the reverse benzoin condensation. In our previous stoichiometric studies involving 1 : 1 triazolium : aldehyde, which were followed to high % product, we investigated the contribution of the reverse reaction for the 2,4,6-trichlorophenyltriazolium tetrafluoroborate salt.[6b] Using two representative substituted benzoins as starting material, <12% retro benzoin reaction was detectable under these conditions over long timescales.

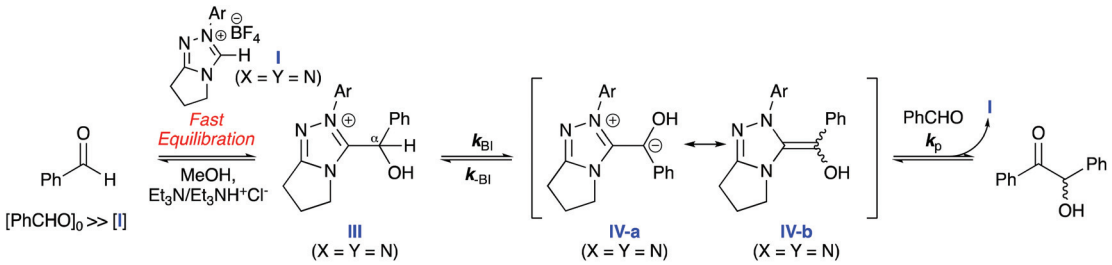

Scheme 2 Key mechanistic steps considered within this kinetic study under catalytic conditions. The initial addition step for formation of **III** has been experimentally shown to occur rapidly and reversibly, with the equilibrium lying significantly towards adduct (**III**) when $[PhCHO]_0$ is in large excess.

Table 1 Summary of the kinetic parameters obtained from fitting experimental data to eqn (2) [a]

Catalyst	[I]/mM	$\nu_{max}/\times10^{-7}$ M s^{-1}	k_{BI}/s^{-1} [c]	k_{BI} (rel)[d]	k_p/k_{-BI}
2a	12	4.08 ± 0.53	3.40×10^{-5}	0.37	5.7
	6	2.27 ± 0.30	3.78×10^{-5}	0.41	5.0
2b	12	6.52 ± 0.49	5.44×10^{-5}	0.59	4.8
2c	24	19.2 ± 3.9	8.02×10^{-5}		1.6
	12	11.1 ± 2.5	9.24×10^{-5}	1.0	2.0
	6	5.52 ± 1.18	9.21×10^{-5}	1.0	2.4
2d	12	16.2 ± 2.1	1.35×10^{-4}	1.5	4.2
2e	12	143 ± 43	1.19×10^{-3}	13	0.94
2f	6[b]	171 ± 3.8	2.85×10^{-3}	31	4.0

[a] Values determined using an initial rate method (IRM) to a maximum of 10% conversion to benzoin product with initial benzaldehyde concentrations ranging from 0.16–1.6 M, in 2 : 1 0.16 M $Et_3N/Et_3NH^+Cl^-$ buffered MeOH solutions at 50 ± 0.01 °C. [b] Reaction in the presence of catalyst **2f** was particularly fast, thus requiring lower loadings to enable study by the IRM. [c] Uncertainties in k_{BI} can be approximated as similar to those in ν_{max}, as $k_{BI} = \nu_{max}/[I]$, with uncertainties in [I] unlikely to have significant impact. [d] k_{BI}(rel) determined as k_{BI}(**2a–f**)/k_{BI} (**2c**) at the same catalyst concentration.

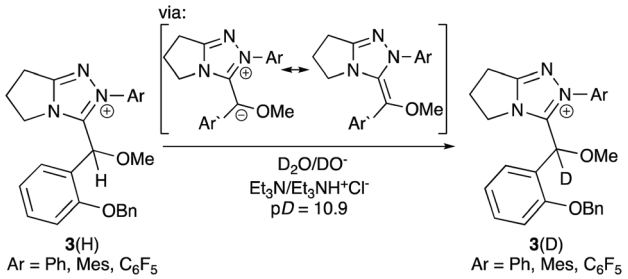

Scheme 3 Previous studies of H/D-exchange of *O*-methylated hydroxyaryl adducts **3** derived from **2b**, **2c** and **2f**.[11] Relative values for k_{ex} (s^{-1}) are similar to k_{BI} (rel) determined herein.

nation to form the Breslow intermediate (**IV**) becomes rate-limiting for triazolium salts **2a–f** at high concentrations of aldehyde. By contrast, as a saturation point is not witnessed within the IRM for thiazolium salt **1**, the formation of Breslow intermediate **IV** does not become cleanly rate-limiting under catalytic conditions in this case. Catalysts **2a** and **2c** were explored at different catalyst concentrations ([I]). Values for the pseudo-first order kinetic constant k_{BI}, determined as $\nu_{max}/[I]$, were consistent within <10% for **2a** and <1% for **2c**, supporting the present kinetic and mechanistic analysis.

Electron withdrawing *N*-aryl substituents are expected to favour formation of Breslow intermediate **IV** from adduct **III** by stabilising the negative charge formed upon deprotonation and thereby increasing the kinetic acidity at the α-position. The observed ν_{max} values are highest for more electron-withdrawing substituents, thus supporting the proposal of rate-limiting formation of **IV** at high $[PhCHO]_0$ and assignment of k_{BI} as the rate constant for this step.

Magnitudes of k_{BI} determined herein are in good agreement with our reported values of k_{ex} for H/D-exchange of *O*-methylated adducts **3** of an *ortho*-substituted aldehyde with the same series of 1,2,4-triazolium catalysts (Scheme 3).[11] *O*-Methylation prevents both reverse equilibration to free aldehyde and catalyst, in addition to onward reaction to benzoin product, thus permitting focus just on the Breslow-intermediate forming step. Although this H/D-exchange study was performed in a predominantly aqueous D_2O medium at a lower temperature of 25 °C, the relative values of k_{ex} and k_{BI} for a given triazolium pre-catalyst are closely similar. Again, this supports our conclusion that the plateau region of the initial rate plots corresponds to the Breslow intermediate (**IV**) forming step and highlights the similarity of triazolium substituent effects in methanol and water media.

Synthetic observations for the benzoin reaction with catalysts **2a–2f** report increased yields of products with more electron withdrawing *N*-aryl substituents.[1a,10b,12] Values for ν_{max} (and k_{BI}) increase with more electron withdrawing *N*-aryl substituents, thus substituent effects on ν_{max} under catalytic conditions correlate with synthetic outcome. An excellent linear Hammett correlation is observed for *para*-substituted catalysts **2a** and **2c–e** with ρ = +1.66 ± 0.05 (Fig. 3).[13] The same Hammett ρ-value is obtained from either log(ν_{max}) or log(k_{BI}) correlations given the common catalyst concentration. Our experimental Hammett ρ-value is intermediary between reference values of ρ = +1.44 and ρ = +3.32 for the acid dissociations of benzoic acids and protonated anilines in methanol, respectively (Fig. 4).[14] This significant sensitivity to substituent change supports the formation of an enaminol-like transition state for the conversion of **III** to **IV** with significant charge neutralisation on the *N*-aryl nitrogen of catalyst in the rate-limiting

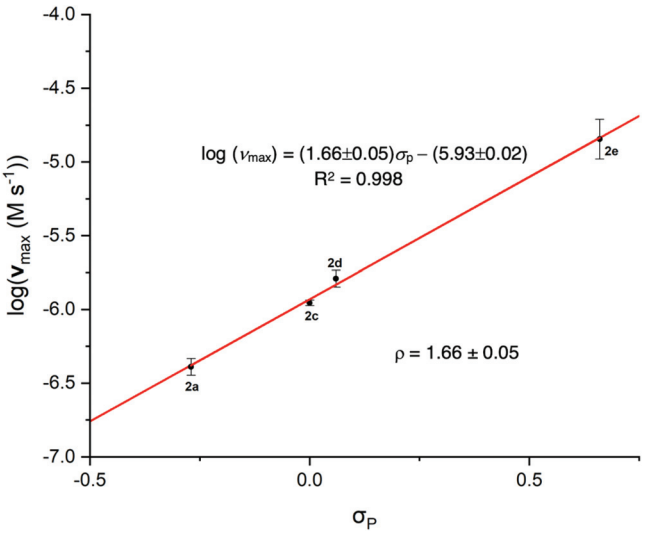

Fig. 3 Triazolium catalysis of the benzoin condensation under catalytic conditions: Hammett correlation of ν_{max} values for *p*-substituted triazolium catalysts **2a** and **2c–e** (12 mM) gives a positive ρ = +1.66. The values for *ortho*-substituted catalysts **2b** and **2f** were excluded from the correlation.

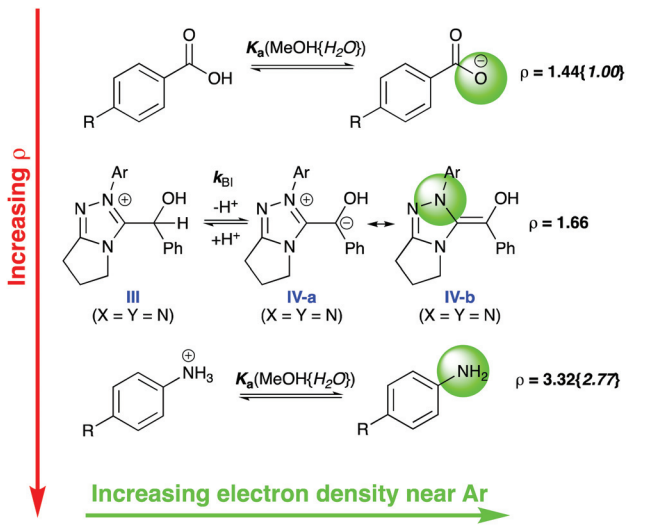

Fig. 4 Comparison of the Hammett ρ values for the reference benzoic acid dissociation (+1.44), the dissociation of anilines (+3.32) and the experimental value obtained herein (+1.66) in methanol {values in braces indicate reference values in water}.[14] Assuming ν_{max} reflects rate-limiting deprotonation of **III** to **IV**, the experimental value for ρ suggests significant increase in electron density near the *N*-aryl substituent in the transition state suggestive of a greater contribution from an enaminol-like resonance canonical structure **IV-b** rather than a more localised carbanion **IV-a**.

step (*cf.* **IV-b**). A significantly smaller Hammett ρ value would be expected for a more localised carbanion-like transition state with charge change more remote from the *N*-Ar of catalyst (*cf.* **IV-a**). The solid state characterisation of Breslow-like intermediates achieved to date (*e.g.* Fig. 1, **IV′**, **IV″**, **IV‴**) also support enaminol-like structures, thus the present Hammett analysis permits unification with behaviour in solution.

Data for *ortho*-substituted triazolium salts **2b** and **2f** were not included in the correlation. Three literature Hammett σ-values have been reported for the pentafluoro-substituent of **2f**, however, there is no reported value for the *N*-mesityl group of **2b**. As is frequently observed owing to the presence of additional steric and electronic factors in *ortho*-substituted cases, the datapoint for **2f** significantly deviates from the correlation line for the *para*-substituted triazolium salts (section S5, ESI†). Irrespective of the Hammett σ-value employed, the log (ν_{max}) value for **2f** falls significantly below the correlation line.

Values of log(k_{BI}/[I]) may also be correlated with pK_as of the triazolium ion pre-catalysts **2a–2f** in both water and DMSO (Fig. S24, ESI†).[6a,10c,d] Although strictly not Brønsted plots, which would require correlation with α-H pK_a values of **III**, these plots serve to demonstrate the increase in k_{BI} with more acidic triazolium pre-catalysts. Harper *et al.* have reported Hammett analyses of pK_a (C3–H) values for three different series of triazolium salts in both water and DMSO.[10d] A Hammett ρ-value of −0.93 ± 0.05 was obtained for the aqueous pK_as of the same family of triazolium catalysts as utilised in the present study with a decrease in pK_a observed for more electron-withdrawing *N*-aryl substituents. Thus, electron-withdrawing *N*-aryl substituents favour acid dissociation of triazolium pre-catalyst in addition to the deprotonation step from adduct **III** to Breslow intermediate **IV**.§

The effect of *N*-aryl substituent on product partitioning of the Breslow intermediate **IV** may also be evaluated by comparison of values for k_p/k_{-BI} obtained from the fit to eqn (2) (Table 1). With the exception of catalyst **2e**, all ratios are greater than 1, suggesting greater contribution from the product benzoin forming step. Values for k_p/k_{-BI} vary in the range 0.94–5.7, with the reliance on two separate kinetic constants being the likely reason for the absence of a clear trend with the electronic nature of the substituent. Interestingly, the highest product ratio is obtained for the most electron-donating *N*-aryl substituent in **2a**, suggesting that the nucleophilicity of **IV** possibly dominates in the benzoin forming step.

Conclusions

In conclusion, a detailed initial rates study of the benzoin condensation using triazolium-ion pre-catalysts under catalytic conditions has been undertaken.[6b] Kinetic behaviour for triazolium salts **2a–2f** under these conditions differ significantly from that of a widely studied thiazolium ion pre-catalyst **1**,

§ Rate constants for proton transfer from **2a–f** to HO^- are in the range 10^6–10^8 M^{-1} s^{-1} and reprotonation of the triazolyl carbene by water has been demonstrated to be close to the diffusional limit for dielectric relaxation of water (10^{11} s^{-1}).[6a] As protonation of diphenyl carbene by methanol has also been shown to be limited by dielectric relaxation of solvent,[15] the proton transfer step between triazolium ions **2a–f** and the corresponding triazolyl carbenes is very unlikely to be rate-limiting in methanol solvent.

with plateauing of the former within the initial rates regime to constant ν_{max} values. Thus, for triazolium pre-catalysts **2a–2f** at low $[PhCHO]_0$, when $k_p[PhCHO] < k_{-BI}$, the reaction appears first-order; conversely, at higher $[PhCHO]_0$, $k_p[PhCHO] > k_{-BI}$ and reaction appears zero-order (eqn (2)). Assignment of the plateau, zero-order region to the Breslow intermediate forming step is supported by: (i) the increase in ν_{max} with electron-withdrawing substituents; (ii) the Hammett plot (Fig. 4), which suggests increase in electron density near the triazolium *N*-Ar group in the rate-limiting transition state; (iii) similar k_{BI}(rel) values and relative k_{ex} values from our previous study of the H/D-exchange reactions of *O*-methylated hydroxyaryl adducts **3**.[11] Conversely, at low [PhCHO], eqn (2) simplifies to rate ∝ [PhCHO], confirming first-order dependence, with contribution to the rate-limiting step from k_p in addition to k_{BI}.

Values for ν_{max} vary greatly depending on the catalyst, with a large 75-fold difference between the slowest **2a** and fastest **2f** triazolium catalysts. These data provide quantitative insight into the role of catalyst *N*-aryl substitution on the rate-limiting step under synthetically-relevant catalytic conditions in a polar solvent environment. In particular, Hammett structure–activity analysis provides evidence for the formation of an enaminol-like transition state **IV-b** for the Breslow intermediate-forming step, permitting the alignment of previous solid state structural characterisation of **IV** with solution state behaviour. With a drive to further the organocatalysis field to more aqueous media, thorough mechanistic analysis in such environments is essential. This work expands our knowledge of the well-explored benzoin condensation, providing mechanistic insight into synthetic observations.

Experimental

Kinetic measurements

Initial benzaldehyde concentrations of 0.32–1.6 M and catalyst loadings of 12 mM, 24 mM and 30 mM were used, in 12.5 mL vials at 50 ± 0.01 °C. Reactions, on a 2.5 mL scale, were initiated by addition of pre-catalyst(**I**) to pre-warmed solutions containing benzaldehyde and the $Et_3N/Et_3NH^+Cl^-$ buffer (0.16 M) and sampled at regular intervals, quenching with acetonitrile and analysing by HPLC.

Conflicts of interest

There are no conflicts to declare.

Acknowledgements

We thank EPSRC [RSM (EP/G013268/1), CJC (EP/G013268/1) and JZ (EP/S020713/1)] and Durham University Doctoral Scholarship Scheme (JM) for funding. We also thank Dr A. Congreve for assistance with HPLC and E. Knighton, A. Davenport and Dr J. Aguilar-Malavia for assistance with NMR studies.

Notes and references

1 (*a*) D. M. Flanigan, F. Romanov-Michailidis, N. A. White and T. Rovis, *Chem. Rev.*, 2015, **115**, 9307–9387; (*b*) M. P. van der Helm, B. Klemm and R. Eelkema, *Nat. Rev. Chem.*, 2019, **3**, 491–508; (*c*) J. Yan, R. Sun, K. Shi, K. Li, L. Yang and G. Zhong, *J. Org. Chem.*, 2018, **83**, 7547–7552; (*d*) C. A. Rose, S. Gundala, C.-L. Fagan, J. F. Franz, S. J. Connon and K. Zeitler, *Chem. Sci.*, 2012, **3**, 735–740; (*e*) J. E. M. Fernando, Y. Nakano, C. Zhang and D. W. Lupton, *Angew. Chem., Int. Ed.*, 2019, **58**, 4007–4011; (*f*) M. S. Kerr, J. Read de Alaniz and T. Rovis, *J. Org. Chem.*, 2005, **70**, 5725–5728; (*g*) C. K. Prier and F. H. Arnold, *J. Am. Chem. Soc.*, 2015, **137**, 13992–14006.

2 (*a*) R. Breslow, *J. Am. Chem. Soc.*, 1958, **80**, 3719–3726; (*b*) R. Breslow and R. Kim, *Tetrahedron Lett.*, 1994, **35**, 699–702.

3 (*a*) T. Dudding and K. N. Houk, *Proc. Natl. Acad. Sci. U. S. A.*, 2004, **101**, 5770–5775; (*b*) S. M. Langdon, C. Y. Legault and M. Gravel, *J. Org. Chem.*, 2015, **80**, 3597–3610; (*c*) Y. He and Y. Xue, *J. Phys. Chem. A*, 2011, **115**, 1408–1417; (*d*) D. A. DiRocco, E. L. Noey, K. N. Houk and T. Rovis, *Angew. Chem., Int. Ed.*, 2012, **51**, 2391–2394.

4 (*a*) B. Maji and H. Mayr, *Angew. Chem., Int. Ed.*, 2012, **51**, 10408–10412; (*b*) D. A. DiRocco, K. M. Oberg and T. Rovis, *J. Am. Chem. Soc.*, 2012, **134**, 6143–6145.

5 (*a*) A. Berkessel, S. Elfert, V. R. Yatham, J. M. Neudorfl, N. E. Schlorer and J. H. Teles, *Angew. Chem., Int. Ed.*, 2012, **51**, 12370–12374; (*b*) M. Paul, P. Sudkaow, A. Wessels, N. E. Schlorer, J. M. Neudorfl and A. Berkessel, *Angew. Chem., Int. Ed.*, 2018, **57**, 8310–8315; (*c*) A. Berkessel, S. Elfert, K. Etzenbach-Effers and J. H. Teles, *Angew. Chem., Int. Ed.*, 2010, **49**, 7120–7124.

6 (*a*) R. S. Massey, C. J. Collett, A. G. Lindsay, A. D. Smith and A. C. O'Donoghue, *J. Am. Chem. Soc.*, 2012, **134**, 20421–20432; (*b*) C. J. Collett, R. S. Massey, J. E. Taylor, O. R. Maguire, A. C. O'Donoghue and A. D. Smith, *Angew. Chem., Int. Ed.*, 2015, **54**, 6887–6892.

7 G. L. Barletta, Y. Zou, W. P. Huskey and F. Jordan, *J. Am. Chem. Soc.*, 1997, **119**, 2356–2362.

8 F. López-Calahorra and R. Rubires, *Tetrahedron*, 1995, **51**, 9713–9728.

9 M. J. White and F. J. Leeper, *J. Org. Chem.*, 2001, **66**, 5124–5131.

10 (*a*) E. M. Higgins, J. A. Sherwood, A. G. Lindsay, J. Armstrong, R. S. Massey, R. W. Alder and A. C. O'Donoghue, *Chem. Commun.*, 2011, **47**, 1559–1561; (*b*) N. Wang, J. Xu and J. K. Lee, *Org. Biomol. Chem.*, 2018, **16**, 8230–8244; (*c*) Z. Li, X. Li and J. P. Cheng, *J. Org. Chem.*, 2017, **82**, 9675–9681; (*d*) N. Konstandaras, M. H. Dunn, M. S. Guerry, C. D. Barnett, M. L. Cole and J. B. Harper, *Org. Biomol. Chem.*, 2020, **18**, 66–75.

11 C. J. Collett, R. S. Massey, O. R. Maguire, A. S. Batsanov, A. C. O'Donoghue and A. D. Smith, *Chem. Sci.*, 2013, **4**, 1514–1522.

12 Y. Niu, N. Wang, A. Munoz, J. Xu, H. Zeng, T. Rovis and J. K. Lee, *J. Am. Chem. Soc.*, 2017, **139**, 14917–14930.

13 C. Hansch, A. Leo and R. W. Taft, *Chem. Rev.*, 1991, **91**, 165–195.
14 (*a*) A. Williams, *Free Energy Relationships in Organic and Bio-Organic Chemistry*, Royal Society of Chemistry, Cambridge, 2003; (*b*) F. Rived, M. Rosés and E. Bosch, *Anal. Chim. Acta*, 1998, **374**, 309–324.
15 J. Peon, D. Polshakov and B. Kohler, *J. Am. Chem. Soc.*, 2002, **124**, 6428–6438.